Research Paper

Complex interrelationships between nitro-alkene-dependent inhibition of soluble epoxide hydrolase, inflammation and tumor growth

Hyun-Ju Cho[a], Christopher Harry Switzer[a], Alisa Kamynina[a], Rebecca Charles[a], Olena Rudyk[b], Tony Ng[c], Joseph Robert Burgoyne[b], Philip Eaton[a,*]

[a] William Harvey Research Institute, Barts and the London School of Medicine, Queen Mary University of London, London, EC1M6BQ, UK
[b] King's College London, School of Cardiovascular Medicine & Sciences, The King's British Heart Foundation Centre of Research Excellence, The Rayne Institute, St Thomas' Hospital, London, SE1 7EH, UK
[c] King's College London, School of Cancer and Pharmaceutical Sciences, Guy's Campus, London, SE1 1UL, UK

ABSTRACT

Nitro-oleate (10-nitro-octadec-9-enoic acid), which inhibits soluble epoxide hydrolase (sEH) by covalently adducting to C521, increases the abundance of epoxyeicosatrienoic acids (EETs) that can be health promoting, for example by lowering blood pressure or their anti-inflammatory actions. However, perhaps consistent with their impact on angiogenesis, increases in EETs may exacerbate progression of some cancers. To assess this, Lewis lung carcinoma (LLc1) cells were exposed to oleate or nitro-oleate, with the latter inhibiting the hydrolase and increasing their proliferation and migration *in vitro*. The enhanced proliferation induced by nitro-oleate was EET-dependent, being attenuated by the ETT-receptor antagonist 14,15-EE-5(Z)-E. LLc1 cells were engineered to stably overexpress wild-type or C521S sEH, with the latter exhibiting resistance to nitro-oleate-dependent hydrolase inhibition and the associated stimulation of tumor growth *in vitro* or *in vivo*. Nitro-oleate also increased migration in endothelial cells isolated from wild-type (WT) mice, but not those from C521S sEH knock-in (KI) transgenic mice genetically modified to render the hydrolase electrophile-resistant. These observations were consistent with nitro-oleate promoting cancer progression, and so the impact of this electrophile was examined *in vivo* again, but this time comparing growth of LLc1 cells expressing constitutive levels of wild-type hydrolase when implanted into WT or KI mice. Nitro-oleate inhibited tumor sEH (P < 0.05), with a trend for elevated plasma 11(12)-EET/DHET and 8(9)EET/DHET (dihydroxyeicosatrienoic acid) ratios when administered to WT, but not KI, mice. Although *in vitro* studies with LLc1 cells supported a role for nitro-oleate in cancer cell proliferation, it failed to significantly stimulate tumor growth in WT mice implanted with the same LLc1 cells *in vivo*, perhaps due to its well-established anti-inflammatory actions. Indeed, pro-inflammatory cytokines were significantly down-regulated in nitro-oleate treated WT mice, potentially countering any impact of the concomitant inhibition of sEH.

1. Introduction

Epoxyeicosatrienoic acids (EETs) are a cytoprotective, health-promoting class of lipids that limit the progression of several diseases [1]. Consistent with this, there have been significant efforts to develop inhibitors of soluble Epoxide Hydrolase (sEH) [1,2], which otherwise degrade EETs to their corresponding dihydroxyeicosatrienoic acids (DHETs) that may lack the protective bioactivity profile of the disease-combatting epoxy lipids. sEH inhibitors offer broad cardiovascular protection, including blockade of smooth muscle cell proliferation and development of atherosclerosis [1,3,4]. Additionally, they are anti-hypertensive and limit the progression of myocardial hypertrophy, heart failure and fibrosis. They also attenuate injury during ischemia in the heart, brain and other organs [5–7].

Nitro-fatty acids, including nitro-oleate, are found endogenously in animals, including humans [8–10]. The classical 'Mediterranean diet'

also supplies nitro-oleate, as well as nitrite- and nitrate-rich vegetables together with unsaturated fats from fish or plants [11]. The nitrite combines with the unsaturated oils in the acidic stomach environment to generate nitro-fatty acids [12]. We previously showed nitro-oleate (10-nitro-octadec-9-enoic acid, NO_2-OA), as well as other lipid electrophiles such as 15-deoxy-prostaglandin J2, adduct to C521 near the catalytic centre of sEH to cause inhibition [13]. The importance of C521 in this inhibition was corroborated by subsequent studies with C521S sEH knock-in (KI) mice engineered to be resistant to hydrolase inhibition by lipid electrophiles [14]. Nitro-oleate increased the EET/DHET ratio, lowered blood pressure and attenuated myocardial hypertrophy in angiotensin II-induced hypertensive wild-type (WT), but not KI, mice. Thus, it was concluded that inhibition of sEH by nitro-oleate explained at least some of the cardiovascular protection by the Mediterranean diet [14], which is rational considering the health-promoting actions of conventional inhibitors of the hydrolase, as outlined above.
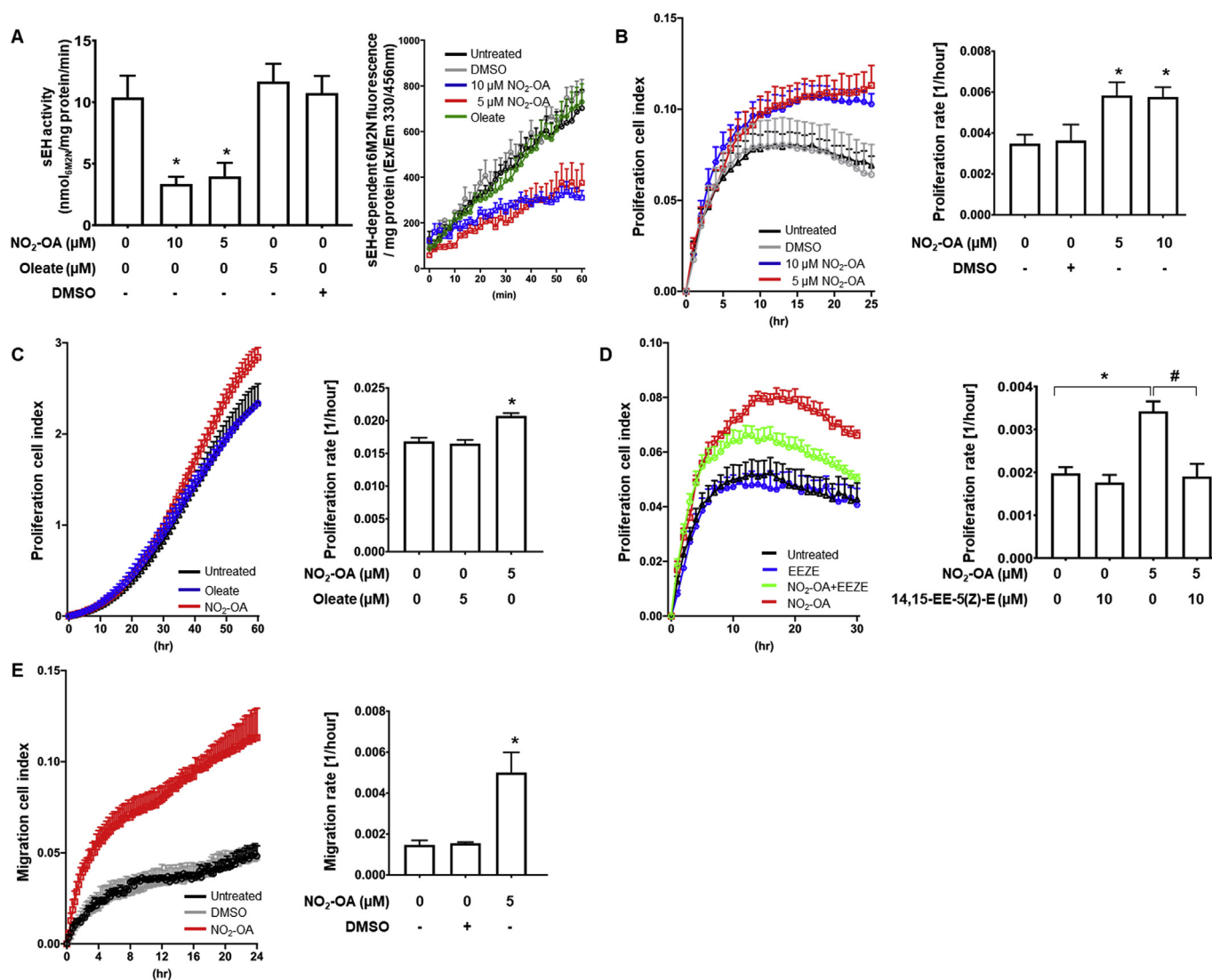
Fig. 1. Nitro-oleate increased proliferation and migration of LLc1 cells through inhibition of sEH and EET signalling

(A) 5 μM or 10 μM nitro-oleate reduced sEH activity. In contrast, sEH activity was not reduced by the non-electrophile oleate (N = 12 per group from 3 independent experiments). The time graph shows that sEH-dependent hydrolysis of PHOME to 6-methoxy-2-naphtaldehyde (6M2N), which is fluorescent, is linear over 60 min. (B-D) Real-time monitoring of LLc1 cell proliferation (cell index) and proliferation rates calculated from these measurements. (B) 5 μM or 10 μM nitro-oleate stimulated proliferation compared to untreated or DMSO-treated control cells (N = 4 independent experiments). (C) In addition, oleate did not stimulate cell proliferation (N = 4 independent experiments). (D) The increased proliferation induced by 5 μM nitro-oleate was normalized by the EET antagonist 14,15-EE-5(Z)-E (N = 4 independent experiments). (E) Real-time monitoring of LLc1 cells trans-well migration (cell index) and migration rates calculated from these measurements. 5 μM nitro-oleate stimulated transmigration compared to untreated or vehicle (DMSO)-treated control cells (N = 4 independent experiments). *P < 0.05 significantly different compared to untreated control. #P < 0.05 significantly different compared to the nitro-oleate treated group.

sEH inhibitors also show therapeutic promise in the treatment of tissue ischemia, perhaps in part because EETs promote angiogenesis and so tissue revascularisation [15]. On the other hand, elevated levels of EETs can also enhance tumor vascularisation and growth *in vivo* [16–19]. Indeed, patients with a history of malignancy are excluded from clinical trials with sEH inhibitors, including recently tested compounds [15]. Elevated dietary nitrite, which may potentially combine with endogenous unsaturated fatty acids to yield nitro-lipid inhibitors of sEH, has been implicated epidemiologically as a risk factor for cancer [20], although there are substantive confounding factors that limit causality being established [21]. Furthermore, there is conflicting evidence that nitro-lipids exert anti-cancer effects, attenuating proliferation and migration of triple negative breast cancer cells [22]. With these considerations in mind, we performed studies to assess whether nitro-oleate can enhance tumor proliferation and growth. The mouse Lewis lung carcinoma cell line (LLc1) cells were selected for study as

there was evidence that exogenously applied EETs enhance their growth *in vivo* when they are implanted in mice [17]. LLc1 cells stably overexpressing sEH, but not C521S sEH, showed potentiated growth in response to nitro-oleate *in vitro* or when engrafted into C57BL/6 mice. In contrast, whilst LLc1 cells expressing constitutive amounts of sEH showed potentiated proliferation in response to nitro-oleate, such a growth enhancement was not observed when these cells were engrafted to WT or KI mice. This may be because the anti-inflammatory actions of nitro-lipids, which may in part be due to their ability to increase ETT levels, may offset their potential for promoting aberrant cancer growth.

2. Material and methods

2.1. Transgenic mice generation and study approval

The KI transgenic mouse line was generated by site-directed

mutagenesis as previously described [13,14]. All procedures were performed in accordance with the Home Office Guidance on the Operation of the Animals (Scientific Procedures) Act 1986 in the United Kingdom and were approved by a King's College London Animal Welfare and Ethical Review Body.

2.2. Cell culture and cell isolation

The LLc1 cell line (ECACC 90020104) was purchased from the European collection of authenticated cell cultures, and cultured in DMEM containing 2 mM L-glutamine, 10% fetal bovine serum and antibiotics (Invitrogen). Mouse aortic endothelial cells (ECs) were isolated from KI or their WT littermates as previously described [23]. Briefly, harvested arteries were digested with 0.05% collagenase type 2 (Gibco) to yield cells that were stained with a CD31 antibody (E-bioscience) and then sorted using a Fluorescence-activated cell sorting Aria II (BD Biosciences). CD31 positive ECs were cultured in the EC growth medium EGM-2MV (Lonza).

2.3. Cell transfection and stable cell line

LLc1 cells were plated in 6-well plates at 50% confluence. The following day cells were transfected with 20 μg of plasmid encoding WT sEH or C521S sEH encoded in a pcDNA 3.1 TOPO Vector (Thermo Fisher Scientific) pre-mixed with Lipofectamine 2000 (Thermo Fisher scientific). To select clones that stably expressed V5-tagged WT or C521S sEH, cells were exposed to geneticin (Thermo Fisher Scientific), which was replaced daily for 10 days. The stability of protein expression was evaluated by immunoblotting using an antibody to sEH (Cayman) and the V5 tag (Abcam), with selected clones expanded for use in subsequent experiments.

2.4. Proliferation and migration assay

For cell proliferation and migration assays, an xCELLigence Real-Time Cell Analyzer DP instrument (ACEA Biosciences) was used. For LLc1 cell proliferation assays, 3000 cells were seeded per well for the experiments shown in Fig. 1B and D, whereas 1000 cells were seeded for that shown in Figs. 1C and 2C. Nitro-oleate, oleic acid (oleate), 12-(3-adamantan-1-yl-ureido)-dodecanoic acid (AUDA), the selective EET antagonist 14,15-Epoxyeicosa-5(Z)-enoic Acid (14,15-EE-5(Z)-E) or dimethyl sulfoxide (DMSO) was mixed with 5% FBS in DMEM. Growth rate was measured automatically every hour. For migration assays, 2×10^4 serum-starved LLc1 cell or ECs were mixed with 5 μM nitro-oleate or DMSO and seeded on the upper chamber of a 16-well CIM-plate (ACEA Biosciences). DMEM or EBM-2 with 2% FBS were loaded in the lower chamber of the CIM-plate and migration rate was measured every 30 min.

2.5. sEH activity assay

Cells treated with nitro-oleate, AUDA or DMSO were harvested and lysed in 0.5% digitonin lysis buffer and centrifuged at 3000 g for 5 min at 4 °C. Whole tumor tissues were homogenized on ice in 100 mM Tris-buffered saline (pH7.4) supplemented with a protease inhibitor cocktail (Roche) using a tissue homogenizer (CAT Scientific) (10% volume/volume). sEH activity was measured using a 3-phenyl-cyano(6-methoxy-2-naphthalenyl)methyl ester-2-oxiraneacetic acid (PHOME, Cayman) as a substrate, which becomes highly fluorescent when its epoxide group is hydrolysed to 6-methoxy-2-naphtaldehyde (6M2N). Cell lysates or tissue homogenates were mixed with or without AUDA to a final concentration 50 μM for 5 min at 37 °C to allow the contribution of sEH to total PHOME hydrolysis to be defined. Subsequently PHOME to a final concentration 20 μM was mixed and fluorescence measurements made at excitation 330/emission 465 nm every 2 min for 1 h using a CLARIOstar plate reader (BMG Labtech) at 37 °C. In some

studies an endpoint assay was performed, making the measurement as above after 1 h. Protein concentration were measured using the bicinchoninic acid assay [13,14,24].

2.6. Aorta ring assay

Thoracic aorta isolated from WT or KI mice were cut into ~2 mm pieces and embed in 96 well plates coated with Matrigel (Corning). Aortas were incubated with 5 μM nitro-oleate or 50 ng/ml vascular endothelial growth factor (VEGF). After 14 days, sprouted vessel length was measured using image J software as before [23].

2.7. Mouse tumor implantation model

1×10^6 LLc1 cells were subsequently injected in WT or KI male mice (12–14 weeks of age). For the study utilising genetically-modified LLc1 cells stably overexpressing WT or C521S sEH, 1×10^5 cells were injected in C57BL/6 mice. After the tumor size reached ~100 mm³, the mice were treated with vehicle (50% saline with 50% DMSO) or 5 mg/kg/day nitro-oleate or oleate using osmotic pumps (ALZET). Tumor volume, which was not allowed to exceed 1.5 cm³, was measured every 2 or 3 days using a calliper. sEH activity and protein expression (Cayman) were measured in harvested tumor tissues. In addition, paraffin-embedded sectioned tumor tissues were stained using Alexa Fluor™ 568 Conjugate isolectin B4 (Thermo Fisher scientific) and DAPI (Sigma). Stained sections were visualized using a Nikon eclipse TS100 fluorescence microscope and isolectin B4 positive cells were counted using Image J software [23]. Plasma was analysed for the EETs and DHETs as described below, and cytokines (interleukin (IL)-1β, IL-6, IL-10 and IL-12p70) analysed using a Bio-Plex multiplex immunoassay kit (Bio-Rad) with a Bio-Plex MAGPIX fluorescence magnetic bead-based immunoassay reader (Bio-Rad) according to the manufacturer's instructions.

2.8. EET and DHET measurement

Plasma samples were prepared in an antioxidant solution comprising 0.2% triphenylphosphine, 0.2% butylated hydroxytoluene and 1% ethylenediaminetetraacetic acid. To isolate lipids, plasma samples (100 μl) were first spiked with 20 ng each of 5(6)-EET-d11, 8(9)-EET-d11, 11(12)-EET-d11,-14(15)-EET-d11, 8(9)-DHET-d11, 11(12)-DHET-d11 and 14(15)DHET-d11 (Cayman), as internals standards and brought to 500 μl with PBS. Next, 2 ml of chloroform: methanol (2:1) was added and the samples were vortexed and centrifuged at 2500 rpm at 10 °C for 10 min. Next the organic phase was transferred to a new tube and dried under nitrogen, after which samples were subject to saponification with 1 ml of 1 M NaOH for 90 min at room temperature. After acidification (pH ~4), lipids were extracted with 4 ml of ethyl acetate, dried under nitrogen and reconstituted in 100 μl of methanol for analysis. Samples were injected (10 μl) into a Shimadzu HPLC with CTC PAL autosampler coupled to a Sciex 5000 triple quadrupole (Sciex). EETs and DHETs were separated on a Phenomenex Luna C18 reversed phase column (2.1 × 100 mm, 5 μm) with Solvent (A) water + 0.1% acetic acid and (B) acetonitrile + 0.1% acetic acid at 0.6 ml/min under the following gradient conditions: 0 min 30%B ramping up to 90%B at 10 min and holding until 15 min followed by a 2 min wash at 100%B and a 3 min equilibration at starting conditions. EETs and DHETs were monitored with the following MRM transitions in negative ion mode: m/z 319.5.191.1 5(6)EET, m/z 330.5.202.1, 5(6)EET-d11, m/z 337.5.145.1 5(6)DHET, m/z 319.5.155.1 8(9)EET, m/z 330.5.167.1 8(9)EET-d11, m/z 337.5.127.1 8(9)DHET, m/z 348.6.127.1 8(9)DHET-d11, m/z 319.5.167.1 11(12)EET, m/z 330.5.167.15 11(12)EET-d11, m/z 337.5.167.1 11(12)DHET, m/z 348.6.167.1 11(12)DHET-d11, m/z 319.5.219.1 14(15)EET, m/z 330.5.219.1 14(15)EET-d11, m/z 337.5.207.1 14(15)DHET, m/z 348.6.207.1 14(15)DHET-d11. EETs and DHETs were quantified using
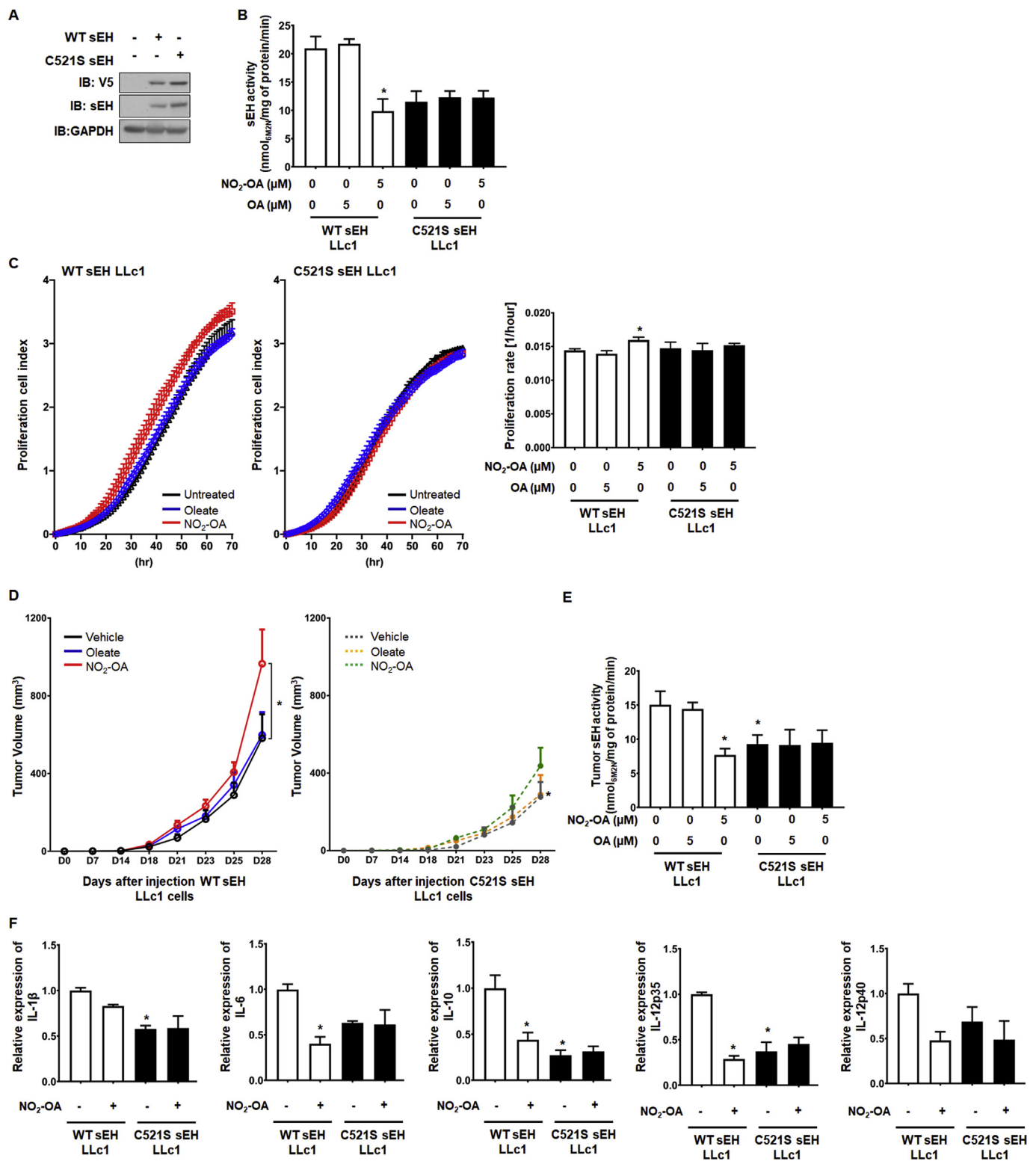
Fig. 2. Nitro-oleate-induced tumor growth is dependent on C521 *in vitro* and *in vivo*

(A) LLc1 cells engineered to stably overexpress WT or C521S sEH do so, as detected by immunoblotting with an antibody to the hydrolase or the V5 tag that the recombinant proteins also carry. The immunoblots are representative of 3 independent experiments. (B-C) 5 μM nitro-oleate decreased sEH activity and stimulated proliferation compared to untreated or oleate-treated LLc1 cells overexpressing WT, but not C521S, sEH (N = 4 independent experiments). *P < 0.05 significantly different compared to untreated WT sEH LLc1 cells. (D-E) 5 mg/kg/day nitro-oleate, oleate or vehicle was administered to mice after their implantation with LLc1 cells overexpressing WT or C521S sEH. Nitro-oleate, but not oleate nor vehicle, stimulated growth in mice with LLc1 cells overexpressing WT, but not C521S, sEH. Nitro-oleate, but not oleate, selectively reduced activity in cells overexpressing the WT hydrolase (N = 6–8 per experimental group from 3 independent experiments). (F) IL-1β, IL-6, IL-10, IL-12p35 and IL-12p40 abundance in tumor tissue was decreased in LLc1 cells overexpressing WT sEH upon exposure to nitro-oleate. These cytokines were lower in abundance basally in tumor tissue derived from cells expressing C521S sEH compared to those overexpressing WT hydrolase. In contrast to tumors originating from cells expressing WT hydrolase, those derived from cells expressing C521S sEH did not change their cytokine abundance when exposed to nitro-oleate (N = 6–8 per experimental group from 3 independent experiments). *P < 0.05 significantly different compared to LLc1 cells expressing WT sEH exposed to vehicle.
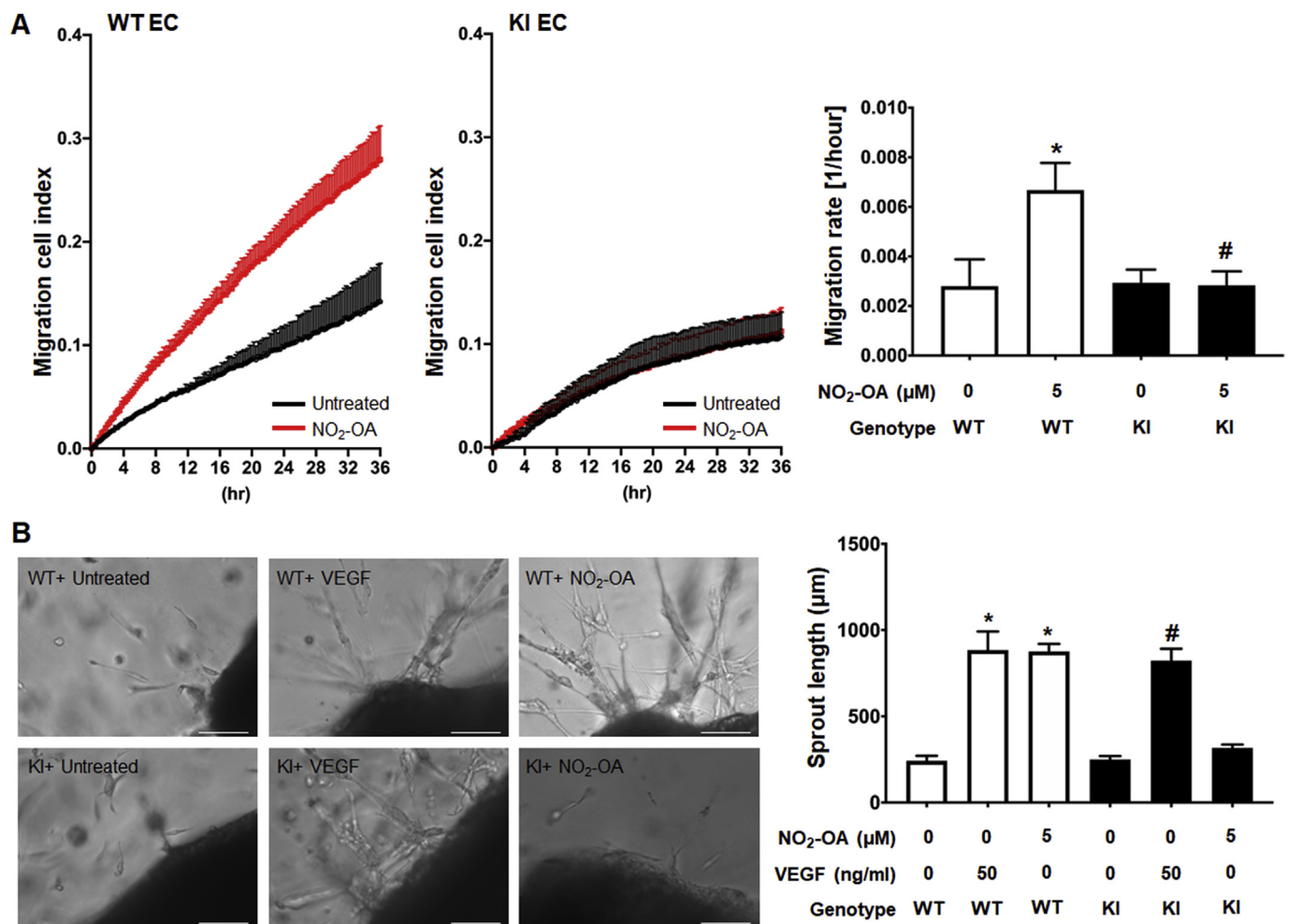
Fig. 3. Nitro-oleate increased migration of ECs from WT but not C521S sEH KI mice.
(A) Real-time monitoring of ECs trans-well migration (cell index) and migration rates calculated from these measurements. 5 μM nitro-oleate stimulated trans-migration in ECs from WT, but not KI, mice compared to untreated controls (N = 4 independent experiments). (B) Representative images from an *ex vivo* vessel sprouting assay and vessel sprout length calculated from these data. Nitro-oleate increased vessel sprout length as much as VEGF in WT but failed to do so in preparations from the KI mice (N = 4 independent experiments). Scale bars show 200 μm *P < 0.001 significantly different compared to untreated WT control, #P < 0.001 significantly different compared to untreated C521 sEH KI control. #P < 0.05 significantly different compared to the nitro-oleate treated WT group.

standard curves of analyte to internal standard. Because no ISTD is available for 5(6)-DHET, the 8(9)-DHET-d11 ISTD was used. EETs and DHETs are reported as a ratio.

2.9. Real-time PCR

Total RNA was extracted from harvested tumor tissues using an RNAesay-Mini Kit (Qiagen), and synthesised complementary DNA (Thermofisher) following the manufacture's protocol. All samples were performed triplicate, and 2 ng cDNA was used with a SYBR-Green (Invitrogen). To measured cytokine expression, IL-1β, IL-6, IL-10, IL-12p35, and IL-12p40 primer were used. cDNA expression were normalized by GAPDH primer was used for the thermal cycler conditions were performed as follows manufacture's manual (Quant Studio 5, Thermofisher). Designed primers were as follows: IL-1β Forward: GAAATGCCACCTTTTTGACAGTG, Reverse: TGGATGCTCTCATCAGGA CAG, IL-6 Forward: GGAGCCCACCAAGAACGATAG, Reverse: GTGAA GTAGGGAAGGCCGTG, IL-10 Forward: GCTGGACAACATACTGCTA ACC, Reverse: ATTTCCGATAAGGCTTGGCAA, IL-12p35 Forward: GGT GAAGACGGCCAGAGAAA, Reverse: GTAGCCAGGCAACTCTCGTT, IL-12p40 Forward: TTCCCTGTCGCTAACTCCCT, Reverse: GTGGAGACAC CAGCAAAACG and GAPDH Forward: AGGTCGGTGTGAACGGATTTG, Reverse: GGGGTCGTTGATGGCAACA (PrimerBank). The relative

mRNA expression levels were normalized with GAPDH and calculated using the 'delta-delta Ct' method.

2.10. Statistical analysis

Difference between groups was calculated by a Student t-test or analysis of variance followed by a Tukey post-hoc test. $P < 0.05$ was considered significantly different.

3. Results

3.1. Nitro-oleate inhibits sEH and increases cancer cell proliferation and migration

5 or 10 μM nitro-oleate, but not the vehicle DMSO, inhibited sEH to a comparable extent to that induced by the established pharmacological hydrolase inhibitor AUDA. In contrast, oleate, which is not electrophilic, did not inhibit sEH (Fig. 1A). Treatment of LLc1 cells with nitro-oleate significantly increased their proliferation rate compared to exposure to vehicle alone or treatment with oleate (Fig. 1B-C). The EET receptor antagonist 14,15-EE-5(Z)-E attenuated the nitro-oleate-induced proliferation of LLc1 cells (Fig. 1D), consistent with the enhanced growth being mediated by increased abundance of EETS that arises due

to electrophilic inhibition of the hydrolase. In addition, 5 μM nitro-oleate dramatically increased migration of LLc1 cells compared to those exposed to vehicle alone (Fig. 1E).

3.2. Nitro-oleate-induced tumor growth is dependent on sEH Cysteine 521

To investigate whether nitro-oleate induced tumor growth by its electrophilic adduction to C521 of sEH, we generated LLc1 cells stably overexpressing WT sEH or C521S sEH. Immunoblotting analysis and sEH activity analysis of whole cell lysates confirmed robust over-expression of active hydrolase in each of the stable cells lines generated (Fig. 2A). Nitro-oleate increased proliferation and decreased sEH activity in LLc1 cells stably overexpressing WT sEH, but not those with the C521S mutant (Fig. 2B-C). LLc1 cells stably overexpressing WT or C521S sEH were implanted into WT C57BL/6 mice and then exposed to nitro-oleate or oleate. LLc1 cells expressing WT sEH exhibited potentiated tumor growth and decreased sEH activity in response to nitro-oleate, but not oleate. However, the LLc1 cells stably overexpressing C521S sEH showed significantly slowed tumor growth compared to sEH LLc1 cell injected group that was not accelerated by nitro-oleate treatment (Fig. 2D-E).

3.3. Nitro-oleate-stimulated EC migration is dependent on sEH Cysteine 521

The increase in migration of LLc1 cell induced by nitro-oleate, a treatment that was also associated with inhibition of sEH, is likely mediated by adduction of the electrophile to C521 of the hydrolase. To test the importance of C521 in the stimulation of cell migration, ECs were isolated from WT or KI mice and exposed to nitro-oleate. Nitro-oleate significantly increased WT EC migration but failed to in cells isolated from the KI mice (Fig. 3A). The impact of nitro-oleate was next assessed using an *ex vivo* aortic ring sprouting assay, comparing the responses of aortic rings isolated from WT to those from KI mice. VEGF, which stimulates angiogenesis in this model and so served as a positive control, increased vessel sprouting to the same extent in vessels isolated from mice of either genotype. In contrast, although nitro-oleate significantly increased sprouting of vessels from WT, this did not occur in those isolated from KI mice (Fig. 3B).

3.4. The impact of nitro-oleate on tumor growth in vivo

It was evident that nitro-oleate stimulated growth and migration of LLc1 cells or ECs, and mechanistically this was at least in part mediated by inhibition of sEH via adduction to C521. However, these conclusions are based on studies with LLc1 cells that overexpressed the hydrolase above levels found constitutively. Consequently, LLc1 cells expressing normal, constitutive amounts of sEH were implanted into WT or KI mice and their growth responses to vehicle or nitro-oleate were determined by serially measuring tumor volume over time. Tumor volume increased over time in all experimental groups (Fig. 4A-C), with a trend towards nitro-oleate enhancing the rate of growth in WT (P = 0.07), whereas it had no such effect in the KI. However, the overall increase in growth was relatively subtle (Fig. 4A), and despite having 12–15 mice per group failed to reach the 5% significance level.

3.5. Nitro-oleate inhibits sEH activity in WT mice and increases EETs

The impact of nitro-oleate on tumor sEH activity and plasma EETs levels was determined 16-days after implantation of LLc1 cells, comparing the response of each genotype to treatment with or without nitro-lipid. Tumor sEH expression was not different between genotypes or altered by exposure to nitro-oleate (Fig. 4D). However, tumor sEH activity in the nitro-oleate treated group was decreased compared to the vehicle treated group in WT mice (P < 0.05), although this was not observed in the xenografts implanted in the KI mice when they were exposed to the electrophile (Fig. 4E). However, although nitro-oleate

reduced sEH activity to a statistically significant extent in tumors implanted in the WT mice, the magnitude of the reduction was rather subtle. In an attempt to gain additional insight to the relationship between tumor growth and sEH activity in mice of either genotype exposed or not to nitro-oleate, correlation analyses were performed (Fig. 4F). Only one experimental group, namely WT mice implanted with a tumor and exposed to nitro-oleate, showed a significant correlation (P < 0.05). The relationship observed showed that in tumor-bearing WT mice treated with nitro-oleate, smaller tumors correlated with higher sEH activity. However, we acknowledge that despite a statistically significant correlation being observed, that the low sample size in these studies limits confidence in these data and so definitive conclusions cannot be drawn. The ratio of 14(15)-, 11(12)-, 8(9)- and 5(6)-EET/DHET was measured in plasma in WT or KI mice harboring tumors exposed to vehicle or nitro-oleate. Although, this analysis did not identify any statistical differences between experimental interventions, it was notable that the WT mice exposed to nitro-oleate showed a trend for increased ratios of plasma 14(15)-, 11(12)- and 8(9)-EET/DHET. However, it should be noted that the KI mice also showed a similar trend towards increased EET/DHET ratios for all measurement performed, with the 14(15)-EET/DHET ratio reaching statistical significance (Fig. 4G). Staining of vascular ECs using isolectin B4 or CD31 as a vascularisation marker showed increased blood vessel density in the nitro-oleate treated group of WT mice, whereas in KI mice this intervention had no impact compared to vehicle control (Fig. 4H).

3.6. Nitro-oleate modulates inflammatory cytokine production

Nitro-oleate is well-established as having anti-inflammatory actions [12,25–28], whereas inflammation is associated with alteration in cytokine profile that may contribute to cancer development [29]. Consequently, plasma and tumor tissue levels of pro-inflammatory cytokines were measured in mice of either genotype implanted with tumors exposed to vehicle or nitro-oleate. Nitro-oleate decreased IL-1β and IL-12 levels in tumor-bearing WT mice compared to vehicle. However, the KI mice that carried tumors had markedly lower levels of several cytokines, namely IL-1β, IL-6, IL-12p70 and IL-10, regardless of whether they had been exposed to vehicle of nitro-oleate (Fig. 4I). These data are consistent with nitro-oleate altering the inflammatory cytokine profile, which may modulate tumor growth, as discussed below.

4. Discussion

The electrophile nitro-oleate inhibited sEH in LLc1 cells, which stimulated proliferation and migration of these lung cancer cells *in vitro*. This mirrors previous studies that showed nitro-oleate, along with some other lipid electrophiles, inhibited hydrolysis of EETs by covalently adducting to Cysteine 521 [14], which is located within the hydrophobic tunnel substrate domain proximal to the hydrolase active site [13]. As the reputed EET-receptor antagonist 14,15-EE-5(Z)-E also attenuated the proliferation stimulated by nitro-oleate, this supported a causal role for EET-induced signalling in the growth response induced by the electrophile. The modification of C521 by nitro-oleate likely causatively mediated the inhibition and enhanced proliferation and migration *in vitro*, as LLc1 cells engineered to stably overexpress C521S sEH that cannot be modified by the electrophile were resistant to these events. In contrast, LLc1 cells stably overexpressing WT sEH responded like normal LLc1 cells with constitutive amounts of the hydrolase to nitro-oleate *in vitro*, namely attenuation of EET hydrolytic activity together with enhanced proliferation and migration. The stable cell lines overexpressing sEH were also studied *in vivo*, by implanting them into C57BL/6 mice and monitoring tumor growth over time. These *in vivo* studies gave comparable results to those with these cells *in vitro*, such that cells overexpressing WT, but not C521S, sEH exhibited potentiated growth in response to nitro-oleate. This promotion of tumor growth *in vitro* as well as *in vivo* by nitro-oleate-dependent inhibition of sEH is
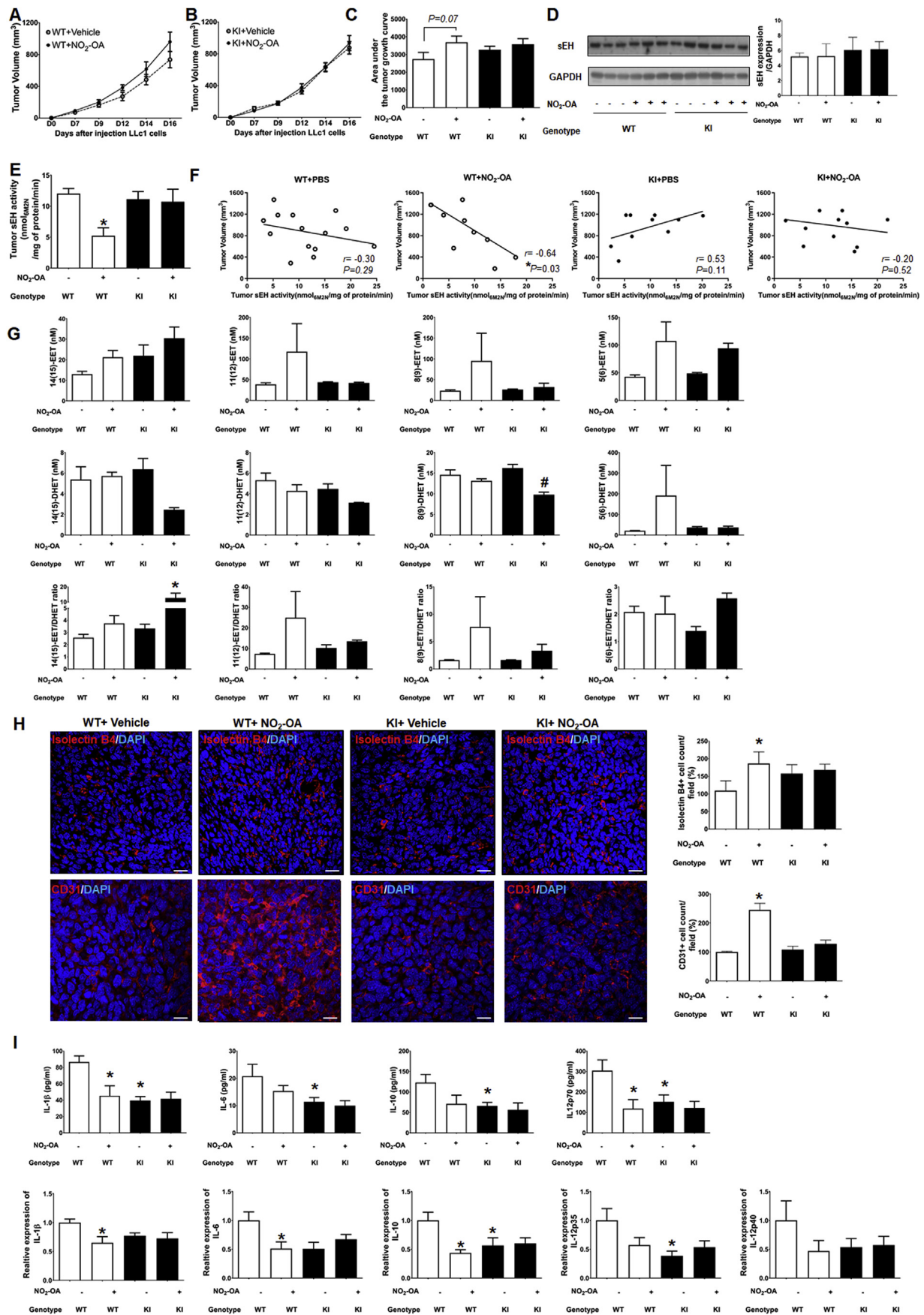
(caption on next page)

Fig. 4. Impact of nitro-oleate on LLc1 tumor growth

(A-C) Temporal measurement of tumor volume in WT or C521S sEH KI mice during treatment with vehicle or 5 mg/kg/day nitro-oleate after implantation with LLc1 cells. The area under the curve for tumor volume was calculated from these data. Nitro-oleate stimulated tumor growth compared to vehicle in WT mice, although this failed to reach statistical significance at the 5% level (P = 0.07). In contrast, there was no difference in tumor volume with or without nitro-oleate treatment in KI mice (N = 12–15 mice were studied per experimental group). (D) Tumor sEH expression was not different between genotypes or altered by nitro-oleate treatment. (E) sEH activity in tumor tissue harvested from WT mice was lower in those from mice exposed to nitro-oleate compared to those only administered vehicle. In contrast, the nitro-lipid did not modulate hydrolase activity present in tumors isolated from KI mice (N = 12–15 mice were studied per experimental group). (F) sEH activity and tumor volume showed a negative correlation in WT mice exposed to nitro-oleate (P < 0.03). This correlative association was absent in KI treated with the nitro-lipid, as well as either genotype administered vehicle alone. (G) EET/DHET ratios in plasma of WT or KI mice treated with or without nitro-oleate. The concentration of plasma the EET/DHET for the 11 (12) or 8 (9) regioisomers showed a trend towards increasing in WT, but not KI, mice harbouring tumors exposed to nitro-oleate (N = 3 mice per experimental group) (H) More isolectin B4 and CD31 positive cells were detected in tumor sections isolated from WT mice exposed to nitro-oleate compared to vehicle. In contrast, nitro-lipid treatment did not increase expression in tumors implanted in C521S sEH KI mice (N = 4 mice per experimental group). (I) Plasma IL-1β and IL-12p70 was significantly decreased in WT mice exposed to nitro-oleate, with a similar downward trend observed for IL-6 and IL-10. This plasma cytokine-lowering by nitro-oleate was not observed in the KI mice, but it was notable they had basally low levels, comparable to those in the vehicle control group (N = 4 mice per experimental group). Cytokine expression in tumor tissue showed a similar trend to their expression in plasma. *P < 0.05 significantly different compared to WT or vehicle control group. #P < 0.05 significantly different compared to vehicle treated KI group. The biochemical and histological analyses reported in panels D-I were performed on samples collected on day 16 of the protocol.

consistent with observations made using other well-established hydrolase inhibitors. For example, *trans*-4-[4-(3-adamantan-1-yl-ureido)-cyclohexyloxy]-benzoic acid (t-AUCB), which reversibly binds the a pair of aspartic acid residues in the active site, is a potent sEH inhibitor that enhanced proliferation and migration of LLc1 cells *in vitro* as well as tumor growth when explanted to mice [17,30]. It was notable that the LLc1 cells expressing WT sEH grew faster when implanted into mice compared to the C521S variant, even in the absence of nitro-oleate, which perhaps reflects differential adduction and inhibition of the hydrolase by endogenous electrophiles.

A limitation of these experiments discussed above was the overexpression of the hydrolase, and so we next compared the growth of LLc1 cells expressing normal levels of sEH, implanting these cells into transgenic C521S sEH mice or their WT controls and comparing tumor growth in response to vehicle or nitro-oleate. Whilst there was a minor trend for nitro-oleate to increase the rate of tumor growth, this was not statistically significant. This failure was despite experimental group sizes of 12–15, providing confidence in the observation. We should consider that the genotype of the murine host is different, but that the tumor cells themselves are identical. Thus, the potential differential responses between genotypes, in which the tumors implanted in KI mice were not stimulated to grow by nitro-oleate, likely reflect disparate responses of the host tissues and not the tumor cells themselves. Once host ECs or immune cells invade the tumor, this would potentially provide a plausible mechanistic explanation for the differential tumor vascularisation and growth responses to nitro-oleate depending on the genotype to which the LLc1 cells were implanted. Indeed, aorta isolated from WT mice showed angiogenic vessel sprouting in response to nitro-oleate, whereas vessels from the KI mice did not. In contrast, vessels from either genotype responded identically to the angiogenesis-stimulator VEGF, consistent with the differential responses to electrophiles in the KI being mediated by modification of C521.

Although nitro-oleate inhibited WT, but not C521S, tumor sEH activity, as may be expected based on the findings so far, there was significant additional complexity. For example, although there was a trend for the nitro-oleate to increase the plasma EET/DHET ratio for the regioisomer pairs measured, this did not reach statistical significance. Furthermore, KI mice also showed a similar trend with the 14(15)-EET/DHET ratio reaching statistical significance, which is notably different than the other observations reported here, in which the C521S mutation renders the hydrolase unresponsive to nitro-oleate. As the tumor cells only express WT sEH, at normal levels, perhaps this explains this observation at least in part, as even when they are implanted to KI mice, their hydrolase can still be inhibited by the nitro-lipid to potentially increase EET abundance. Ideally, we would also have measured other metabolic products of EETs, as well as plasma EETs and DHETs in mice that were not implanted with tumors, but this was not possible for us. We should also consider that EETs abundance are modulated by several

pathways in addition to sEH that generates DHETs. These include metabolism by β- or ω-oxidation, as well as by phospholipase or cyclooxygenase [31–34]. EETs can also esterified, with the free, unesterified forms accounting for ~3% of rat plasma EETs [35]. This esterification may decrease the abundance and signalling processes associated with free EETs [31]. Although esterified EETs can have regulatory functions themselves, such as ion transport control [36,37], a complete understanding remains to be elucidated [38]. In addition, the relationship between esterified EETs and cancer progression is also incompletely understood. Herein we have specifically focused on conversion of EETs to DHETs and hydrolase activity. In this connection, whilst a sEH inhibitor increased tumor size [17], co-administration of the cyclooxygenase-2 inhibitor celecoxib dramatically attenuated this growth response [30,34,39]. Consistent with this, 4-(5-phenyl-3-(3-3-(4-trifluoromethyl-phenyl)-ureido)-propyl)-pyrazol-1-yl)-benzenesulfonamide (PTUPB), which inhibits both sEH and cyclooxygenase, synergistically suppressed tumor growth [34,40] and potentiated the anticancer effect of cisplatin [41]. It seems clear that sEH inhibition combined with anti-inflammatory interventions can afford synergistic anticancer activities. As nitro-lipids inhibit sEH as well as anti-inflammatory actions, this may explain the lack of a statistically significant increase in LLc1 tumor growth *in vivo*. The anti-inflammatory actions are mediated at least in part by attenuating formation of cyclooxygenase-derived proangiogenic metabolites of EETs [34]. Inhibition of sEH alone would generate more substrates for formation of these proangiogenic metabolites, but inhibition of cyclooxygenase-2 would attenuate their formation and limit cancer growth.

Correlation analysis of the relationship between sEH activity and tumor size at the end of the protocol was performed for each of the four experimental groups, namely mice of either genotype administered vehicle or nitro-oleate. Notably, this showed that there was a statistically significant relationship only in one of these four groups, namely the WT mice exposed to nitro-oleate – with bigger tumors being associated with lower hydrolase activity. These analyses showed again that nitro-oleate inhibited sEH and this was associated, perhaps causatively considering the data presented here in its entirety, with enhanced tumor growth. Panigraphy et al. showed sEH expression was reduced to a greater extent in larger tumors over 5 cm^3, with no alteration in expression in those smaller than 1 cm^3 [17]. In our study, sEH expression changes were not detected. However, because of mouse welfare considerations tumors were not allowed to develop beyond 1.5 cm^3 and so cannot be directly compared to this previous study.

Besides inhibiting sEH activity, nitro-oleate can also exert anti-inflammatory actions, with several studies study showing it lowered the abundance of the cytokines IL-1β, IL-6 and IL-12 induced by exposure to lipopolysaccharide or IL-4, although other anti-inflammatory cytokines such TGFβ and IL-10 were also downregulated [25,27,28]. In addition, sEH inhibition also has a strong anti-inflammatory action

through increasing abundance of EETs. For example, mice treated with the sEH inhibitor AUDA showed significantly reduced inflammation when exposed to lipopolysaccharide [42]. In the studies reported here, nitro-oleate reduced the expression of pro-inflammatory IL-1β, IL-6 and IL-12. As these cytokines have been shown to mediate tumor growth [43–45], it is possible, as considered above, that this anti-inflammatory action of the nitro-lipid counters growth potentiation arising from sEH inhibition and increased angiogenic EETs. This may explain why the nitro-lipid did not significantly increase growth of tumors implanted into WT mice. Woodcock et al. showed that nitro-oleate reduced triple-negative breast tumor growth [22], which was attributed to its anti-inflammatory, as they like us observed a reduction in cytokines. Whilst we did not see a reduction in LLc1 tumor growth upon exposure to nitro-oleate, there were differences in its dose, route and duration of administration, which together with etiological differences between disparate cancers, makes direct comparisons difficult. It is also notable that samples from patient with triple-negative breast cancer had high levels of EETs and lower amounts of sEH compared to those from triple-positive controls [46]. Furthermore, EETs stimulated triple-negative breast tumor growth via activating the phosphoinositide 3-kinase-protein kinase-B pathway [19].

5. Conclusion

In conclusion, C521-dependent inhibition of sEH by nitro-oleate robustly promoted proliferation and migration of ECs or LLc1 cells *in vitro*. However, when the LLc1 cancer cells were implanted into mice, there was not clear evidence of growth promotion induced by the nitro-lipid, which may be due to the anti-inflammatory actions it concomitantly exerted.

Funding

Declaration of competing interest

None of the authors have any conflicts of interest to declare.

Acknowledgements

Appendix A. Supplementary data

Supplementary data to this article can be found online at https://doi.org/10.1016/j.redox.2019.101405.

References

[1] J.D. Imig, B.D. Hammock, Soluble epoxide hydrolase as a therapeutic target for cardiovascular diseases, Nat. Rev. Drug Discov. 8 (10) (2009) 794–805.

[2] A.A. Spector, Arachidonic acid cytochrome P450 epoxygenase pathway, J. Lipid Res. 50 (Suppl) (2009) S52–S56.

[3] J.D. Imig, Epoxide hydrolase and epoxygenase metabolites as therapeutic targets for renal diseases, Am. J. Physiol. Renal. Physiol. 289 (3) (2005) F496–F503.

[4] J.D. Imig, Epoxides and soluble epoxide hydrolase in cardiovascular physiology, Physiol. Rev. 92 (1) (2012) 101–130.

[5] D. Xu, et al., Prevention and reversal of cardiac hypertrophy by soluble epoxide hydrolase inhibitors, Proc. Natl. Acad. Sci. 103 (49) (2006) 18733–18738.

[6] J. Monti, et al., Soluble epoxide hydrolase is a susceptibility factor for heart failure in a rat model of human disease, Nat. Genet. 40 (2008) 529.

[7] D. Ai, et al., Soluble epoxide hydrolase plays an essential role in angiotensin II-induced cardiac hypertrophy, Proc. Natl. Acad. Sci. 106 (2) (2009) 564–569.

[8] D. Tsikas, et al., Nitro-fatty acids occur in human plasma in the picomolar range: a targeted nitro-lipidomics GC-MS/MS study, Lipids 44 (9) (2009) 855–865.

[9] S.R. Salvatore, et al., Characterization and quantification of endogenous fatty acid nitroalkene metabolites in human urine, J. Lipid Res. 54 (7) (2013) 1998–2009.

[10] M. Delmastro-Greenwood, et al., Nitrite and nitrate-dependent generation of anti-inflammatory fatty acid nitroalkenes, Free Radic. Biol. Med. 89 (2015) 333–341.

[11] M. Grossi, et al., A novel electrochemical method for olive oil acidity determination, Microelectron. J. 45 (12) (2014) 1701–1707.

[12] B.A. Freeman, et al., Nitro-fatty acid formation and signaling, J. Biol. Chem. 283 (23) (2008) 15515–15519.

[13] R.L. Charles, et al., Redox regulation of soluble epoxide hydrolase by 15-deoxy-delta-prostaglandin J2 controls coronary hypoxic vasodilation, Circ. Res. 108 (3) (2011) 324–334.

[14] R.L. Charles, et al., Protection from hypertension in mice by the Mediterranean diet is mediated by nitr inhibition of soluble epoxide hydrolase, Proc. Natl. Acad. Sci. U. S. A. 111 (22) (2014) 8167–8172.

[15] A.L. Lazaar, et al., Pharmacokinetics, pharmacodynamics and adverse event profile of GSK2256294, a novel soluble epoxide hydrolase inhibitor, Br. J. Clin. Pharmacol. 81 (5) (2016) 971–979.

[16] D. Panigrahy, et al., EET signaling in cancer, Cancer Metastasis Rev. 30 (2011) 525–540 0.

[17] D. Panigrahy, et al., Epoxyeicosanoids stimulate multiorgan metastasis and tumor dormancy escape in mice, J. Clin. Investig. 122 (1) (2012) 178–191.

[18] J. Luo, et al., 14,15-EET induces the infiltration and tumor-promoting function of neutrophils to trigger the growth of minimal dormant metastases, Oncotarget 7 (28) (2016) 43324–43336.

[19] J. Luo, et al., 14, 15-EET induces breast cancer cell EMT and cisplatin resistance by up-regulating integrin alphavbeta3 and activating FAK/PI3K/AKT signaling, J. Exp. Clin. Cancer Res. 37 (1) (2018) 23.

[20] A. Etemadi, et al., Mortality from different causes associated with meat, heme iron, nitrates, and nitrites in the NIH-AARP Diet and Health Study: population based cohort study, BMJ 357 (2017) j1957.

[21] S. Rohrmann, J. Linseisen, Processed meat: the real villain? Proc. Nutr. Soc. 75 (3) (2015) 233–241.

[22] C.C. Woodcock, et al., Nitro-fatty acid inhibition of triple-negative breast cancer cell viability, migration, invasion, and tumor growth, J. Biol. Chem. 293 (4) (2018) 1120–1137.

[23] J.R. Burgoyne, et al., Deficient angiogenesis in redox-dead Cys17Ser PKARIalpha knock-in mice, Nat. Commun. 6 (2015) 7920.

[24] C. Morisseau, B.D. Hammock, Measurement of soluble epoxide hydrolase (sEH) activity, Curr. Protoc. Toxicol. 4 (4 23) (2007).

[25] A.T. Reddy, S.P. Lakshmi, R.C. Reddy, The nitrated fatty acid 10-Nitro-oleate diminishes severity of LPS-induced acute lung injury in mice, PPAR Res. 2012 (2012) 617063.

[26] H. Rubbo, Nitro-fatty acids: novel anti-inflammatory lipid mediators, Braz. J. Med. Biol. Res. 46 (9) (2013) 728–734.

[27] G. Ambrozova, et al., Nitro-oleic acid modulates classical and regulatory activation of macrophages and their involvement in pro-fibrotic responses, Free Radic. Biol. Med. 90 (2016) 252–260.

[28] R.A. Isidro, C.B. Appleyard, Colonic macrophage polarization in homeostasis, inflammation, and cancer, Am. J. Physiol. Gastrointest. Liver Physiol. 311 (1) (2016) G59–G73.

[29] M. Esquivel-Velazquez, et al., The role of cytokines in breast cancer development and progression, J. Interferon Cytokine Res. 35 (1) (2015) 1–16.

[30] G. Zhang, et al., Dual inhibition of cyclooxygenase-2 and soluble epoxide hydrolase synergistically suppresses primary tumor growth and metastasis, Proc. Natl. Acad. Sci. U. S. A. 111 (30) (2014) 11127–11132.

[31] W.B. Campbell, et al., Orally active epoxyeicosatrienoic acid analogs, J. Cardiovasc. Pharmacol. 70 (4) (2017) 211–224.

[32] A.A. Spector, et al., Epoxyeicosatrienoic acids (EETs): metabolism and biochemical function, Prog. Lipid Res. 43 (1) (2004) 55–90.

[33] L. Yang, et al., The role of epoxyeicosatrienoic acids in the cardiovascular system, Br. J. Clin. Pharmacol. 80 (1) (2015) 28–44.

[34] A.A. Rand, et al., Cyclooxygenase-derived proangiogenic metabolites of epoxyeicosatrienoic acids, Proc. Natl. Acad. Sci. U. S. A. 114 (17) (2017) 4370–4375.

[35] H. Jiang, G.D. Anderson, J.C. McGiff, Red blood cells (RBCs), epoxyeicosatrienoic acids (EETs) and adenosine triphosphate (ATP), Pharmacol. Rep. 62 (3) (2010) 468–474.

[36] A. Karara, et al., Endogenous epoxyeicosatrienoyl-phospholipids. A novel class of cellular glycerolipids containing epoxidized arachidonate moieties, J. Biol. Chem. 266 (12) (1991) 7561–7569.

[37] J. Chen, et al., Inhibition of cardiac L-type calcium channels by epoxyeicosatrienoic acids, Mol. Pharmacol. 55 (2) (1999) 288–295.

[38] V. Sudhahar, S. Shaw, J.D. Imig, Epoxyeicosatrienoic acid analogs and vascular function, Curr. Med. Chem. 17 (12) (2010) 1181–1190.

[39] K.M. Wagner, et al., Soluble epoxide hydrolase as a therapeutic target for pain, inflammatory and neurodegenerative diseases, Pharmacol. Ther. 180 (2017) 62–76.

[40] A. Gartung, et al., Suppression of chemotherapy-induced cytokine/lipid mediator surge and ovarian cancer by a dual COX-2/sEH inhibitor, Proc. Natl. Acad. Sci. U. S. A. 116 (5) (2019) 1698–1703.

[41] F. Wang, et al., COX-2/sEH dual inhibitor PTUPB potentiates the antitumor efficacy of cisplatin, Mol. Cancer Ther. 17 (2) (2018) 474–483.

[42] S. Norwood, et al., Epoxyeicosatrienoic acids and soluble epoxide hydrolase: potential therapeutic targets for inflammation and its induced carcinogenesis, Am. J. Tourism Res. 2 (4) (2010) 447–457.

[43] G. Trinchieri, Interleukin-12 and the regulation of innate resistance and adaptive immunity, Nat. Rev. Immunol. 3 (2) (2003) 133–146.

[44] R.N. Apte, et al., The involvement of IL-1 in tumorigenesis, tumor invasiveness, metastasis and tumor-host interactions, Cancer Metastasis Rev. 25 (3) (2006) 387–408.

[45] S. Tugues, et al., New insights into IL-12-mediated tumor suppression, Cell Death Differ. 22 (2) (2015) 237–246.

[46] M.K. Apaya, et al., Integrated omics-based pathway analyses uncover CYP epoxygenase-associated networks as theranostic targets for metastatic triple negative breast cancer, J. Exp. Clin. Cancer Res. 38 (1) (2019) 187.